Functionalization of textile cotton fabric with reduced graphene oxide/MnO₂/polyaniline based electrode for supercapacitor

Functionalization of Textile cotton fabric with reduced graphene oxide/MnO_2/polyaniline based electrode for supercapacitor

Bulcha Belay Etana[1,2], Shanmugam Ramakrishnan[2], Dhakshnamoorthy M[1,2*], Saravanan S[2], Praveen C. Ramamurthy[2*], Tamene Adugna Demissie[1]

[1]School of Materials Science and Engineering, Jimma Institute of Technology, Jimma University, Jimma, P.O.Box.378, Ethiopia.

[2]Department of Materials Engineering, Indian Institute of Science, Bangalore, India.

[1*]Address for Correspondence, E-mail: dhakshnamoorthy.mani@ju.edu.et, Tel: +251 906191022

[2*]Address for Correspondence, E-mail: praveen@iisc.ac.in, Tel:+91-80-2293-2627

Abstract

In this work, a new cotton electrode has been synthesized by coating ternary materials of reduced graphene oxide (rGO), manganese dioxide (MnO_2), and polyaniline (PANi) on textile cotton fabric. First, Graphene oxide was deposited on cotton fibers by a simple "dip and dry" method and chemically reduced into rGO/cotton fabric. MnO_2 nanoparticles were accumulated on rGO/cotton fabric by *in-situ* chemical deposition method. PANi layer was coated on rGO/MnO_2/cotton fabric by *in-situ* oxidative polymerization technique. A thin PANi coating layer acts as a protective layer on rGO/MnO_2/cotton fabric to restrain MnO_2 nanoparticles and rGO from dissolution in H_2SO_4 acidic electrolyte. The specific surface area of cotton electrode was measured using the Brenauer-Emmett-Teller (BET) method. The cyclic voltammetry (CV) results show that the cotton electrode has good capacitive behavior. The ternary cotton electrode exhibits high specific capacitance values of 888 F g^{-1} and 252 F g^{-1} at a discharge current density of 1 A g^{-1} and 25 A g^{-1} in 1 M H_2SO_4 electrolyte solution. The high areal specific capacitance of 444 Fcm^{-2} was achieved for as-fabricated electrode. Also, the cotton electrode retains around 70% of specific capacitance after 3000 cycles at charge-discharge current density of 15 A g^{-1}. The slow decrease in specific capacitance is observed with increased discharge current density which proves its excellent rate capability. These results of rGO/MnO_2/PANi/cotton fabric electrode show that this can be an excellent electrode for supercapacitor in energy storage devices.

Key Words: Reduced graphene oxide, Manganese dioxide, Polyaniline, Cotton fabric electrode, Supercapacitor

1. Introduction

From the past decade, the smart wearable energy storage devices have been extensively investigated by the researchers. In smart textiles, cotton fabrics are particularly used as flexible materials. [1-5] The electrically conductive materials such as carbon nanomaterials (e.g. graphene, carbon nanotubes), [6] the materials with high electrochemical properties such as metal oxide nanoparticles (MnO_2, NiO, Cu_2O, TiO_2, Fe_3O_4, etc.), [7, 8] and conducting polymers (PANi, [9-11] PPy, [12] polythiophene, [13] etc.) are being utilized to enhance the electrochemical properties of textile electrodes. These electrodes are used in supercapacitors for energy storage device applications.

Briefly, a supercapacitor is an electrochemical device which can store high energy (electric charges) and release current density and capacitance within a short time interval. There are two categories of supercapacitors available: they are electric double layer capacitors (EDLC) and psuedocapacitors based on the charge storage mechanism. In EDLC, the storage of charge is achieved by separating electronic and ionic charges in the electrode and electrolyte interface. Alternatively, psuedocapacitors store charges by *Faradaic* reactions occur in the active materials of the electrodes. The carbon based materials are most common electrode for EDLCs. However, EDLCs are limited to low energy storage density. The conducting polymers and metal oxides can store greater amounts of energy in psuedocapacitors compared to an EDLC. [14] Many researchers are still working on the electrodes to enhance the electrochemical properties of the supercapacitors.

The functionalization of cotton fabric with graphene material can impart the electrical conductivity. The hydroxyl groups present on the cotton fiber surface provide active sites for functionalization with many additives which include graphene, graphene oxide, and carbon nanotubes. [15-17] The addition of graphene oxide onto cotton fabric leads to bind easily with

the surface of fibers through interaction between the polar groups present on both cotton fiber and graphene oxide. There has been many research investigations reported on a flexible and light weight rGO/cotton fabric electrode based macroscopic supercapacitor. The electrode was fabricated by a combination of simple "dipping and drying" method. [18-20]

The transition metal oxides, MnO_2, TiO_2, and CuO [8, 21] have been proved that they can be used as electrodes for supercapacitors. In particular, MnO_2 has its own advantages such eco-friendliness, low cost, high theoretical specific capacitance of 1230 $mAhg^{-1}$, and favorable cycling stability. [7] Xiao et al. prepared carbon fabric composite electrode by chemically anchoring metal oxide nanoparticles (MnO_2, SnO_2, and RuO_2)onto graphenenanosheets. [8] The prepared composite was coated over carbon fabric. The incorporation of MnO_2 nanoparticles improved the electrochemical performance. The cotton fabric surface contains exogenous groups which facilitates the uniform deposition rGOnanosheets and MnO_2 nanoparticles. Also, the uniform deposition prevents aggregation of rGO and MnO_2 nanoparticles. [22-23]

In recent years, many investigations have been attempted on cotton based pseudocapacitors by coating conducting polymers, mainly polyaniline (PANi), polypyrrole (PPy), [24-25] and polythiophene [13]. Specifically, Polyaniline (PANi) has been extensively investigated in supercapacitor application because of its excellent theoretical specific capacitance of 2000 Fg^{-1} compared to polypyrrole. However, PANi has poor cycling stability which leads to rapid decrease of specific capacitance and resulting in short cycle life. Many research works have been carried out by the researchers to fabricate different PANi based composites by incorporating with carbon based nanomaterials and metal oxides for improving electrochemical properties such as specific capacitance and charge-discharge cycle stability of the electrode. [24]

More recently, the composite electrodes have attracted researchers due to improvement in the electrochemical properties of electrodes. [26-29] Particularly, a combination of carbon based nanomaterials, metal oxide nanoparticles, and conducting polymers has attracted the researchers due to their potential for achieving excellent specific capacitance. The rGO/PANi [30-36] and rGO/MnO_2 cotton electrodes belong to binary composite electrode material. [37-38] The addition

of conducting polymer to rGO/MnO_2 composite cotton electrode will further enhance the specific capacitance. [39]

In this work, we prepared a ternary composite based cotton fabric electrode material for the first time in the supercapacitor application which consists of reduced graphene oxide (rGO), manganese dioxide (MnO_2) and polyaniline (PANi). The electrochemical properties of developed cotton fabric electrode were studied. The addition of rGO and PANi improve the electrochemical properties of cotton fabric electrodes. Also, metal oxide coated rGO increases the capacitance and cycling stability of the electrode. The combination of these materials together increase electrochemical properties such as specific capacitance, charge-discharge cycle stability and also energy density of the cotton fabric electrode.

2. Experimental

2.1. Materials

Commercial woven cotton fabric (100%) samples of 120 g m^{-2} were obtained from Ethiopian Textiles Company and the fabrics were desized and cleaned according to conventional procedure. Graphite flakes was bought from Sigma-Aldrich Chemicals. Sulphuric acid (H_2SO_4), Hydrochloric acid (HCl), Sodium Nitrate ($NaNO_3$), Hydrogen peroxide (H_2O_2 30%), Potassium permanganate ($KMnO_4$) powder, Manganese sulfate ($MnSO_4$), Sodium hydroxide (NaOH) pellets, Aniline, Ammonium peroxodisulfate (APS), Sodium borohydride ($NaBH_4$), and N-Methyl-2-Pyrrolidone (NMP) solvent were supplied by Spectrochem, India.

2.2. Synthesis of Graphene Oxide (GO)

Graphene oxide was synthesized from pure graphite flakes by a modified Hummer's method as reported in our previous work [40]. Briefly, 1.2 g of Graphite flakes and 2 g of $NaNO_3$, were mixed with 50 ml of H_2SO_4 in a volumetric flask (500 ml) kept in an ice bath with continuous stirring for 2 h. Then, 6 g of $KMnO_4$ was added very slowly for about 1 hr due to exothermic oxidation reaction. The slow addition leads to intercalation of functional groups due to oxidation

of graphene layer which resulted in formation of graphitic oxide. After the addition of $KMnO_4$, the mixture was diluted by adding 100 ml of de-ionized water into the mixture. The reaction temperature was quickly increased to 90°C and the sample mixture was stirred continuously for 24 hrs. Then, the mixture became brownish paste like material. The increase in temperature led to the exfoliation of graphite oxide into graphene oxide. Then, 8 ml of H_2O_2 (30%) was added slowly to the mixture to react completely with the excess $KMnO_4$ under stirring. After 10 minutes, a bright yellow solution was obtained and it was then kept without stirring for 4 hrs, where the particles settled at the bottom and remaining solution was poured. The resulting mixture was washed repeatedly with 5% HCl solution several times to remove the metal ions from the solution and decanted the upper liquid part. Then, the mixture was washed many times with de-ionized (DI) water until the solution's pH becomes neutral. Finally, the solution was filtered and the paste like material was dried in vacuum oven at 60°C for 12 hrs. The dried graphene oxide (GO) was ground into powder.

2.3. Fabrication of rGO/MnO_2/PANi coated Cotton fabrics

The textile cotton fabrics are highly flexible, low cost and commercially available for clothing. However, cotton cannot be used as flexible electrode due to its insulating and low electrochemical activity. Functionalization of cotton fabric with electrically conductive and pseudocapacitance materials is necessary to achieve its electrochemical performance. [16]

The commercial cotton fabrics have number of impurities which include dirt, seed coat fragments, pesticides, chemical residues, metallic salts and immature fibers. Among the various pretreatments of cellulosic textile materials, only scouring (cleaning) employ an alkaline agent in concentrated solution. The scouring or boiling-off process permits the removal of certain impurities with which the fiber is associated. The white plain woven cotton fabrics (120 gm^{-2}) was pretreated by dipping in NaOH (40 gL^{-1}) aqueous solution at 80 °C for 1 h. The GO suspension ink was prepared by dissolving 2 mg of GO powder in 150 mL of de-ionized water under ultra-sonication for 30 mins. The 2 cm^2 with 0.02 cm thickness size of pretreated cotton fabric was dipped into a GO suspension ink and soaked for 30 minutes to coat GO on to the cotton fabric and then vacuum dried at 60°C for 1 hrs. The dip-coating process was repeated for

several times to achieve more GO adsorption on cotton fabric. The obtained GO/cotton fabric was partially reduced into rGO/cotton fabric, by a chemical method using aqueous solution of $NaBH_4$. The chemical reduction process was carried out by immersing GO/cotton fabric in an aqueous solution of $NaBH_4$ (0.1 M) for about 5 hrs under continuous stirring condition. The obtained rGO/cotton fabric was washed with de-ionized water and then vacuum dried at 70°C for 6 hrs. The electrostatic interaction, van der Waals' force and hydrogen bonding between cotton fabric and partial rGO facilitates the uniform coat and adhesion forces between them.

The prepared rGO/cotton fabric was immersed into a 250 mL flask containing 45 mL of 0.02 mol $MnSO_4$ aqueous solution and kept stirring for 15 minutes. Then, 30 mL of 0.02 mol $KMnO_4$ aqueous solution was added drop wise into the reaction mixture by stirring continuous for 6 hrs at room temperature. The color of rGO/cotton fabric turned from purple to brown which indicated the deposition of MnO_2 nano particles on the surface of rGO/cotton fabric. The obtained rGO/MnO_2/cotton fabric (grayish blue) was then washed five times with de-ionized water to remove residual reactants and vacuum dried at 50°C for 4 hrs. The mass loading of MnO_2 was calculated from the difference in mass of rGO/cotton fabric and rGO/MnO_2/cotton fabric electrodes.

Polyaniline was deposited onto the rGO/MnO_2/cotton fabric by *in-situ* chemical polymerization of aniline. In a typical process, rGO/MnO_2 cotton fabric electrode (2 cm^2) was immersed in 50 mL of de-ionized water and stirred the solution for 15 min to ensure that it was fully wet. Then, aniline (0.2 mol L^{-1}) was added into the mixture containing 1 M HCl (10 mL) and was stirred for 2h. The oxidant, aqueous solution of ammonium persulfate (10 mL:0.2 M in 1 M HCl) was added to carry out the oxidative polymerization under continuous stirring. The *in-situ* oxidative polymerization leads to coating of PANi on the rGO/MnO_2 cotton fabric electrode surface.

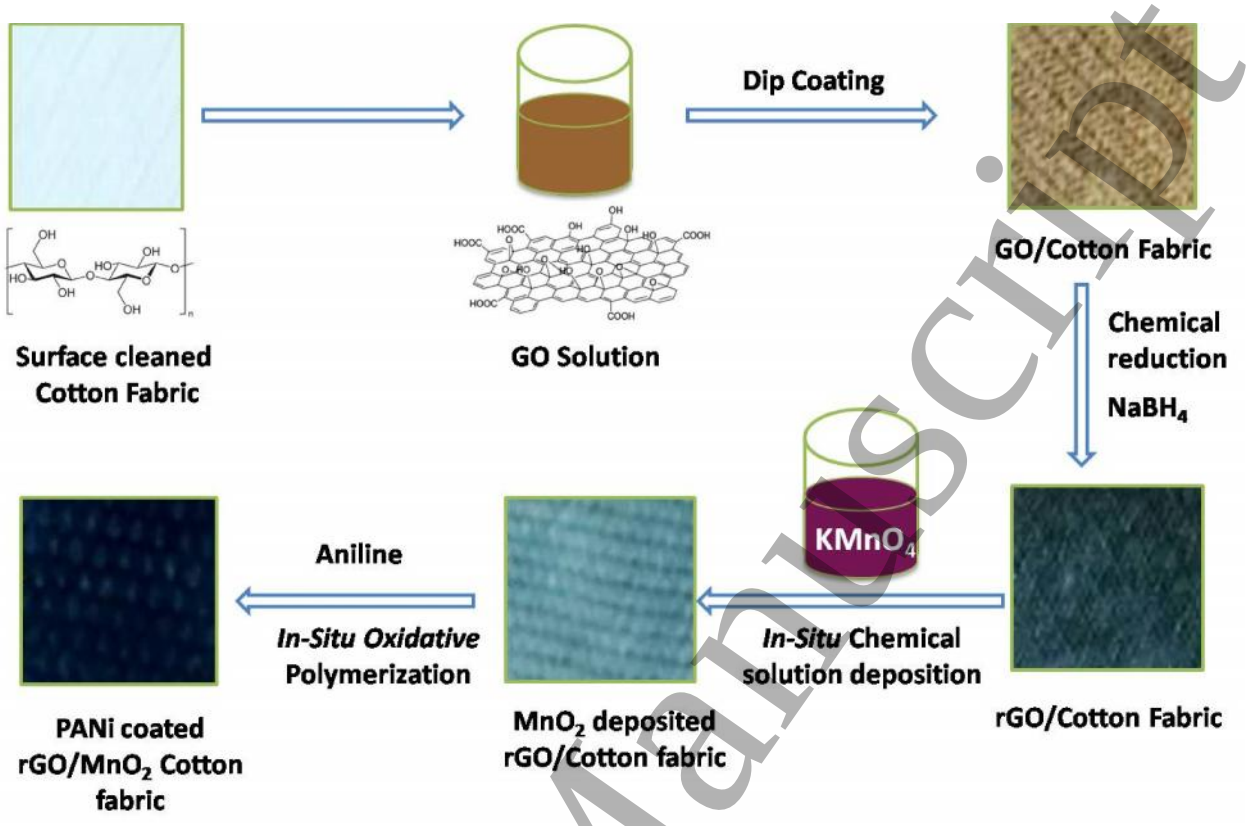

Fig.1. The schematic synthesis roadmap of rGO/MnO_2/PANi/cotton fabric electrode

The reaction was carried out for 14 h and the color changed to bluish black and rGO/MnO_2/PANi/cotton fabric was separated and washed with mixture of de-ionized water and ethanol for four times. The product was dried in a vacuum oven at 50 °C for 10 h to obtain rGO/MnO_2/PANi/cotton fabric electrode. The schematic synthesis roadmap of rGO/MnO2/PANi/cotton fabric electrode is shown in Fig.1.

The change in color was identified which may be induced by the functionalization of cotton fabrics with rGO, MnO_2 nanoparticles, and PANi. Fig.2. shows the white LED lighted up by connecting the ternary coated cotton fabric electrode with electric voltage. The white LED connected to the prepared cotton electrode and electric voltage. LED light was glowing when electric current was passed through the cotton electrode.

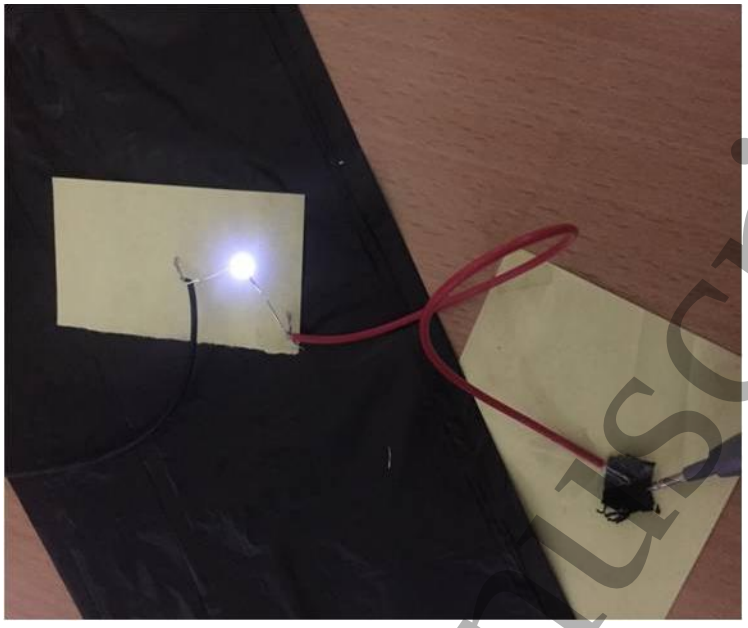

Fig.2. Digital photograph of white LED lighted up by connecting rGO/MnO_2/PANi/cotton fabric electrode with electric voltage

2.4. Characterization

Fourier transform infrared (FTIR) spectroscopic results were obtained for different samples from a Perkin Elmer (Lambda 35) FTIR spectrometer with an ATR transmission mode in the wavelength range of 400 – 4000 cm^{-1}. Raman spectroscopy was conducted by Horiba JobinYvon t6400 instrument using a 532 nm laser source and in transmission mode in the wavelength range of 400 – 3000 cm^{-1}. The X-ray diffraction (XRD) data were obtained with Cu K_α radiation (λ = 0.1541 nm), an accelerating potential of 40 kV and 30 mA at a scanning rate of 0.5 °/min on a Rigaku X-ray diffractometer. The Surface morphology of coated cotton fabrics with gold sputtered (5nm) was investigated by Field Emission Scanning electron microscope (FESEM, Carl Zeiss Ultra 55) at accelerating voltage of 10 kV with energy and angle selective backscattered electron (EsB) detector. The elemental analysis was carried out by High-Angle Annular Dark-Field Scanning Transmission Electron Microscopic (HAADF-STEM) method using a JEOL 2100F microscope at 200 kV operating voltage. The specific surface area, pore volume and pore size of the electrode samples were measured by Brunauer–Emmett–Teller (BET) method with a BELSORP-mini II instrument. Electrochemical measurements, cyclic

voltammetry (CV), Galvanostatic charge-discahrge cycle were studied by an Electrochemical Analyzer (Autolab-Ecochemie, Netherlands).

3. Results and Discussion

3.1. Structure characterization of rGO/MnO_2/PANi/cotton fabrics

FTIR spectra of untreated and surface treated cotton fabrics are shown in Fig.3. Cellulose characteristic peaks of 3275 cm^{-1} and 2915 cm^{-1} were assigned to C=O stretching vibrations and C–O stretching vibrations of the cellulose chains respectively.

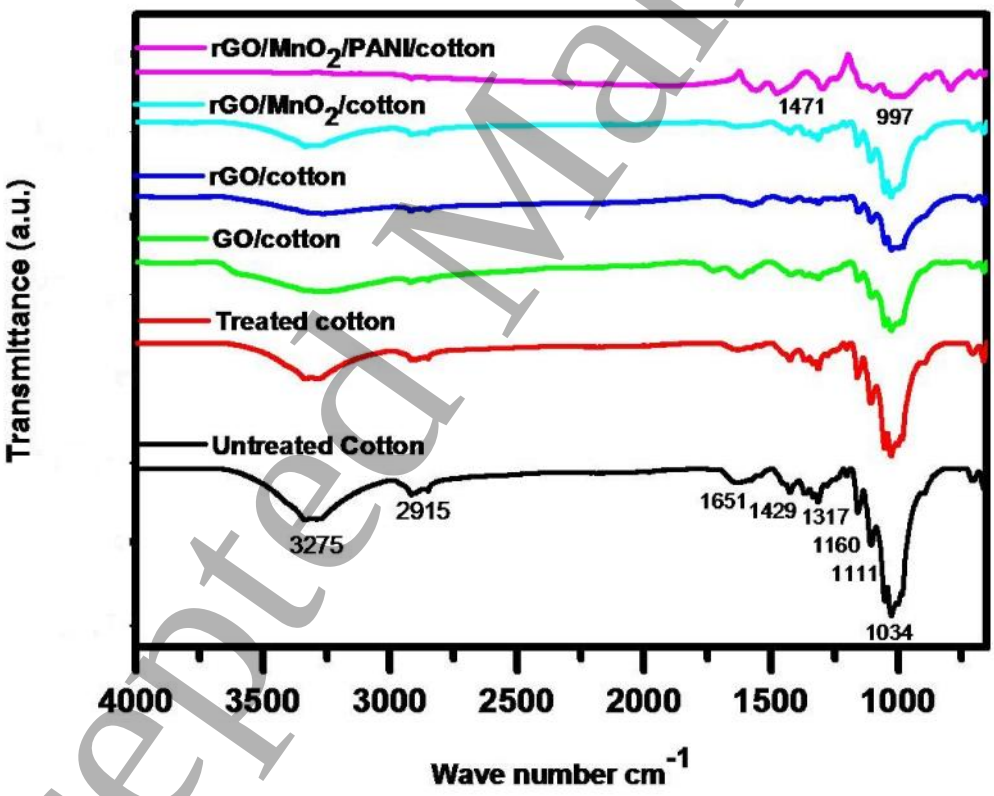

Fig.3. FTIR spectra of GO, rGO, rGO/MnO_2 and rGO/MnO_2/ PANi cotton fabrics.

The GO coated cotton showed the characteristic peaks at 1728 cm^{-1} (carbonyl C=O), 1619 cm^{-1} (aromatic C=C), 1399 cm^{-1} (carboxyl O=C–O), 1218 cm^{-1} (epoxy C–O–), and 1038 cm^{-1} (alkoxy

C–O) stretching vibrations. The Peak at 1728 cm^{-1} was disappear in rGO and rGO/MnO_2 coated cotton fabrics which confirmed the reduction of GO to rGO. The peak for MnO_2 was observed at 1034 cm^{-1} attributed to Mn–O vibrations, which reveals that MnO_2 nanoparticles are present in rGO/MnO_2 and rGO/MnO_2/PANicoated cotton fabrics. The characteristic peaks at 4275 and 1317 cm^{-1} correspond to –O–H stretching and bending vibrations respectively. The FTIR spectrum of rGO/MnO_2/PANIi coated cotton fabric showed that the characteristic peak of PANi at 1573 cm^{-1} due to stretching of quinonoid, peak at 1471 cm^{-1} due to stretching of benzenoid rings, and at 1296 cm^{-1} due to C–N stretching. The characteristic peaks at 1317 cm^{-1} and 1118 cm^{-1} are due to C=N stretching and bending vibrations of the aromatic C–H observed at 811cm^{-1}.

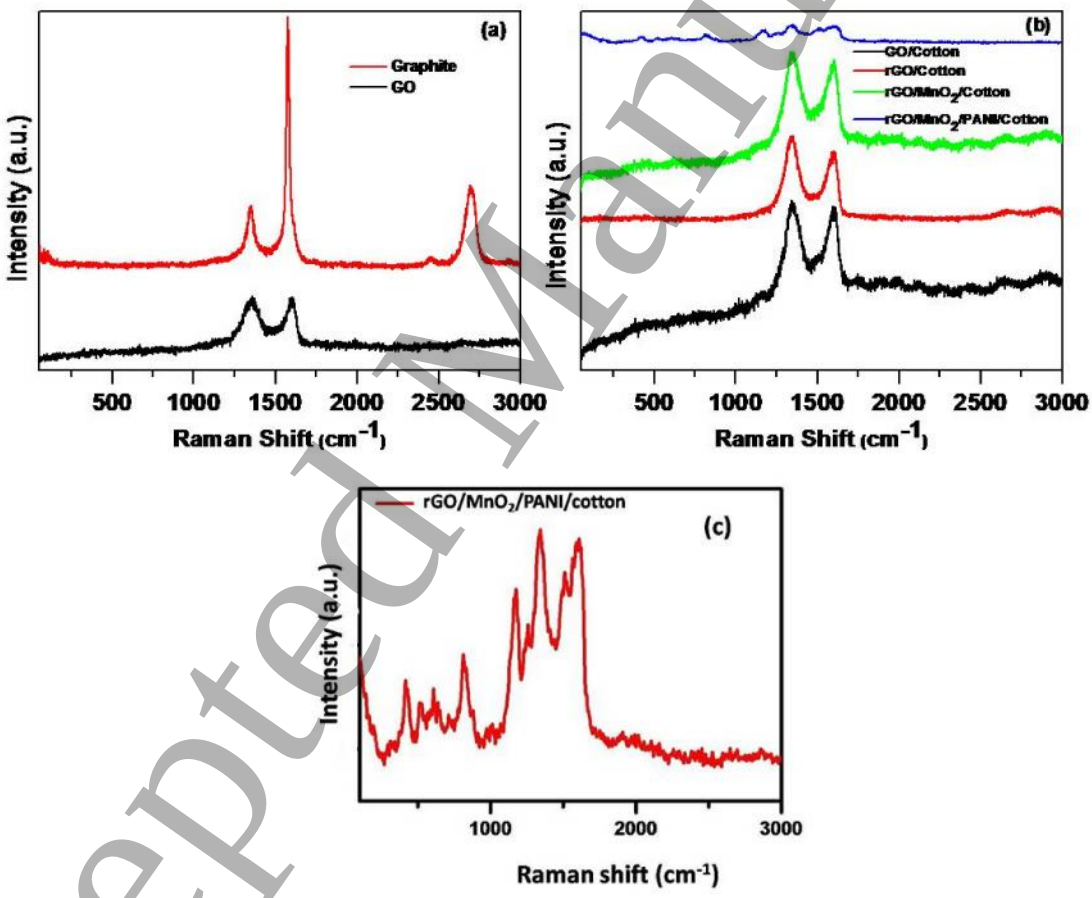

Fig.4. Raman Spectra of (a) Graphite and GO, (b) GO, rGO, rGO/MnO_2 and rGO/MnO_2/ PANi coated Cotton, and (c) detailed spectrum of rGO/MnO_2/ PANi coated Cotton.

Functionalization of graphite into graphene oxide was confirmed by Raman spectroscopy. Fig.4.(a) shows Raman spectra of graphite and graphene oxide and Fig.4.(b) shows for

GO/Cotton, rGO/cotton, rGO/MnO_2/cotton, and rGO/MnO_2/PANi cotton. The GO exhibited a defect D-band due to carbon disorder at 1351.1 cm^{-1} and a peak appeared at 1602.7 cm^{-1} corresponds to shifted graphitic G-band due to sp^2–bonded carbon as compared with graphite (1573cm^{-1}). A broad shifted 2G–band observed due to phonon double resonance at 2765 cm^{-1} for graphite and this peak was disappeared in GO. The intensity ratio of the I_D/I_G was high compared to GO and other samples (GO/Cotton, rGO/cotton, rGO/MnO_2/cotton, and rGO/MnO_2/PANi cotton. Figure.4. (c) shows the detailed Raman spectrum of rGO/MnO_2/PANi/cotton and D-band & G-band are observed but with a shift from 1345 cm^{-1}, and from 1613 cm^{-1} bending vibration of the quinonoid units, and C=C stretching vibration in the quinonoid ring respectively.

The peaks at 1334, 1223, 1485 and 1585 cm^{-1} are associated with vibrations of the semi-quinone and C–N stretching mode of polaronic unit. Table.1. shows the list of Raman spectral peak positions, intensity and I_D/I_G ratios of GO, GO/cotton, rGO/cotton, rGO/MnO_2/cotton, and rGO/MnO_2/PANi/cotton fabric samples.

Table. 1. List of Raman spectra peak positions, intensities, and I_D/I_G ratios of different samples

Sample	D-band position (cm^{-1})	D-band intensity	G-band position (cm^{-1})	G-band intensity	I_D/I_G ratio
GO	1351.10	270.90	1602.70	267.21	1.040
GO/cotton	1341.82	870.10	1602.70	848.20	1.027
rGO/cotton	1347.06	1122.12	1597.47	1060.18	1.060
rGO/MnO_2/cotton	1341.82	1448.18	1607.60	1412.40	1.025
rGO/MnO_2/PANI/cotton	1338.10	186.04	1592.81	183.16	1.016

The peak intensity ratio observed from rGO/cotton is calculated to be 1.06 which is slightly higher than GO/cotton i.e., 1.027. The increase in I_D/I_G ratio from 1.027 to 1.060 confirmed the reduction of GO to rGO. It can be attributed to a decrease in the average size of the sp^2 domains

due to reduction of GO and also an increase in the fraction of graphene edges. After functionalization of MnO_2 with rGO, the peaks at 1347.06 cm^{-1} and 1597.47cm^{-1} for rGO shifted to 1341.82 cm^{-1} and 1607.6 cm^{-1} and in the case of rGO-MnO_2 also the intensity ratio has changed from 1.06 to 1.025 due to the suppression of vibrating species of MnO_2 surpasses the rGO band through stokes effect. This confirms the bonding of MnO_2 functionalization over the rGO surface and at the same time it can be inferred that the incorporation and intercalation of MnO_2 molecules intern to facilitates the π-π conjugation in PANi which in turn leads to the composite with good conductivity.

X-ray diffraction patterns of GO, rGO/cotton, rGO/MnO_2/cotton, and rGO/MnO_2/PANi/cotton are shown in Fig.5. (a). The XRD pattern of MnO_2 (Fig. 5. (b)) was similar to that of Figure (a) with additional peaks at 14.65 and 16.37 which indicate that there is an *in-situ* growth of MnO_2 layer on the rGO/cotton surface. The diffraction peaks at 15.17 and 16.86 of 2θ value in the XRD pattern of rGO/MnO_2/PANi/cotton also confirm that PANi covered the cotton fibers completely. The XRD pattern of MnO_2 nano particles prepared by *in-situ* deposition method is provided in Figure. 5. (b). It shows sharp peaks 2θ at 37.17° and 66.29°, which correspond to crystalline α-MnO_2. Also, the appearance of broad peaks may be due to the partial presence of amorphous α-MnO_2.

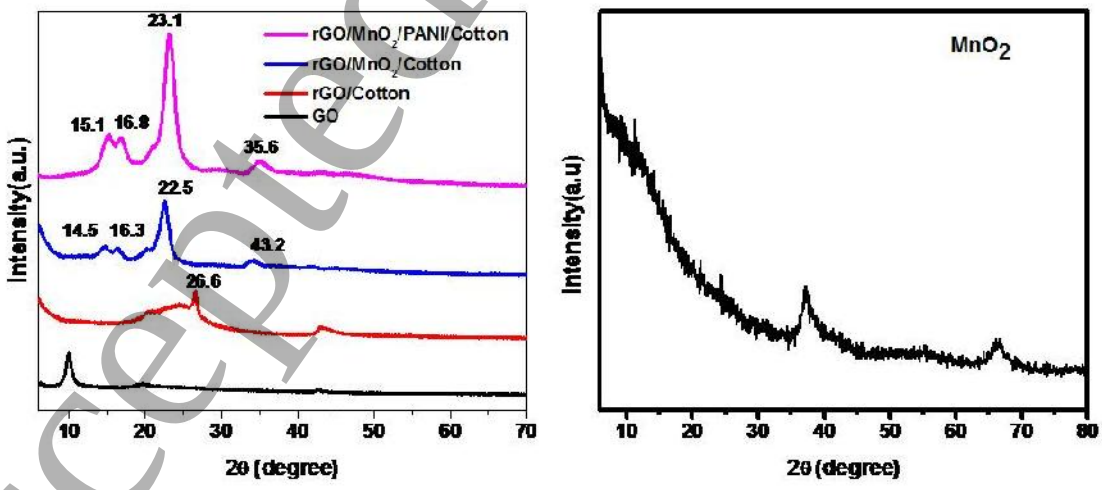

Fig.5. X-ray diffraction pattern of (a) GO, rGO/cotton, rGO/MnO_2/cotton, and rGO/MnO_2/PANi/cotton, (b) MnO_2

3.2. Morphology and structure of synthesized ternary rGO/MnO2/PANi cotton fabrics

Scanning electron microscopic images of pure surface treated cotton (Fig.6. (a, b)) and GO coated cotton showed in Fig.6. (c, d). It is shown in Fig.6. (c, d) that GO layers coated on the cotton fiber surface. After reduction of GO/cotton fabric, the presence of rGO sheets is clearly shown in Fig.7. (a, b). In Fig.7. (c, d), It can be seen that PANi was attached completely to rGO, when the rGO/cotton fabric was dipped fully into the polymerization reaction solution of aniline. MnO_2 nano particles were coated on rGO/cotton textile fibers by mixing rGO/cotton fabric with $KMnO_4$, Mn (VII) is reduced into spherical nano particles of MnO_2 coated on rGO/cotton which is shown in Fig. 8. (a, b). Due to high density, MnO_2 layer was coated at low concentration to facilitate electrolyte ion permeation.

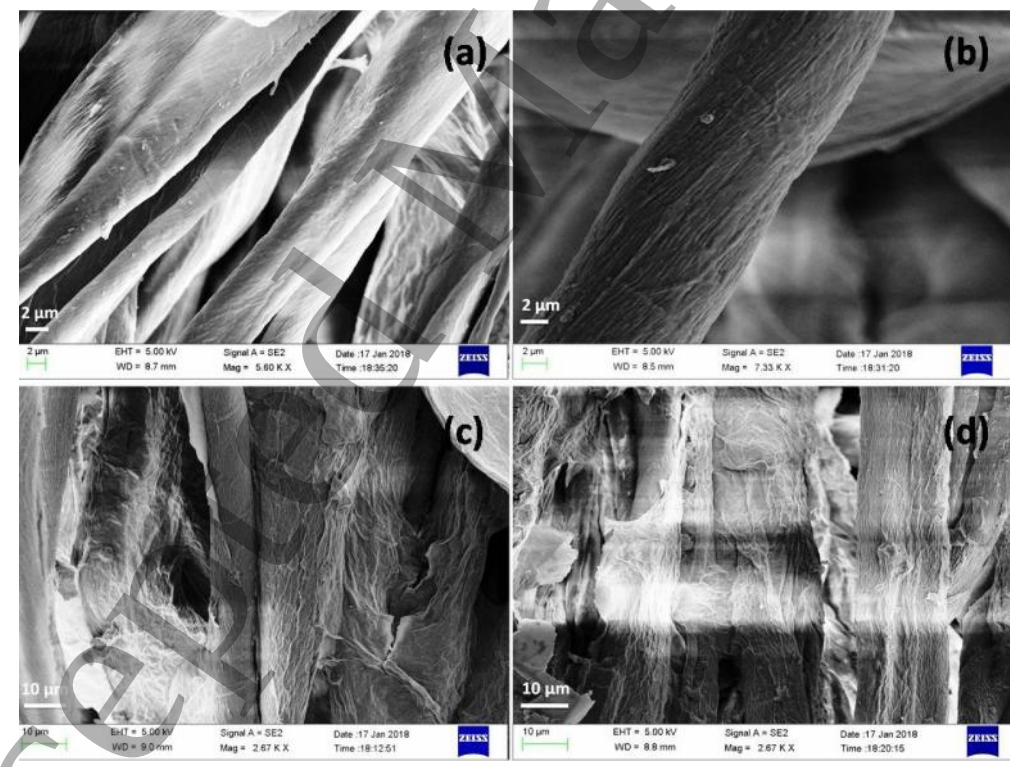

Fig.6. FE-SEM images of (a, b) pure surface treated cotton, and (c, d) GO coated cotton fabrics

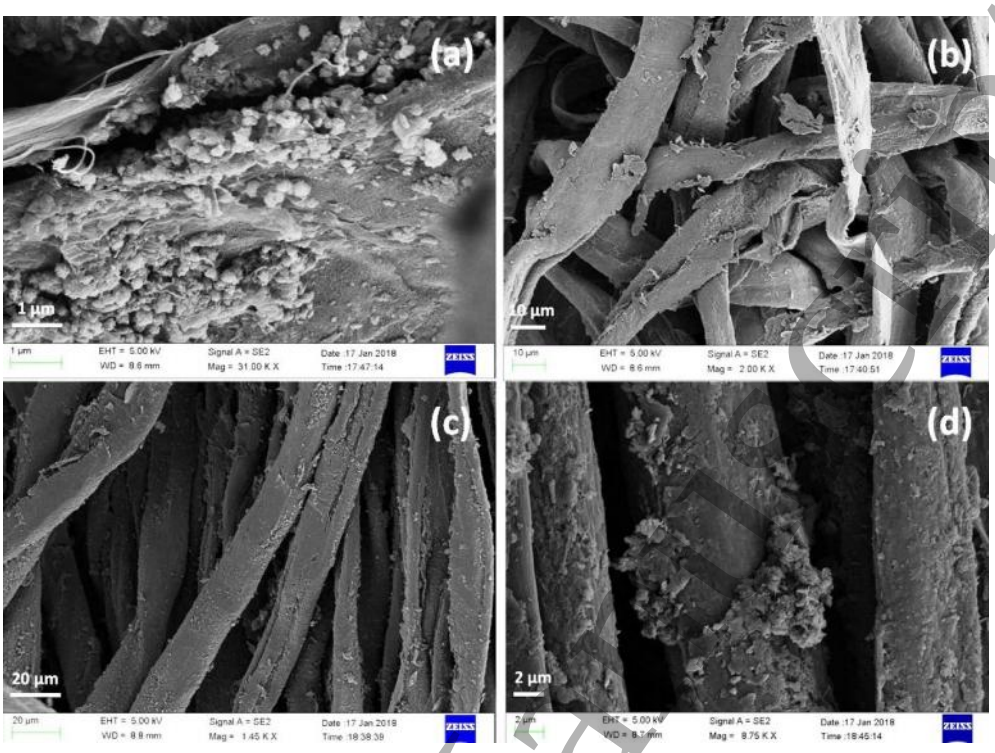

Fig.7. FE-SEM images of (a, b) rGO/cotton, and (c, d) rGO/PANi coated cotton fabrics

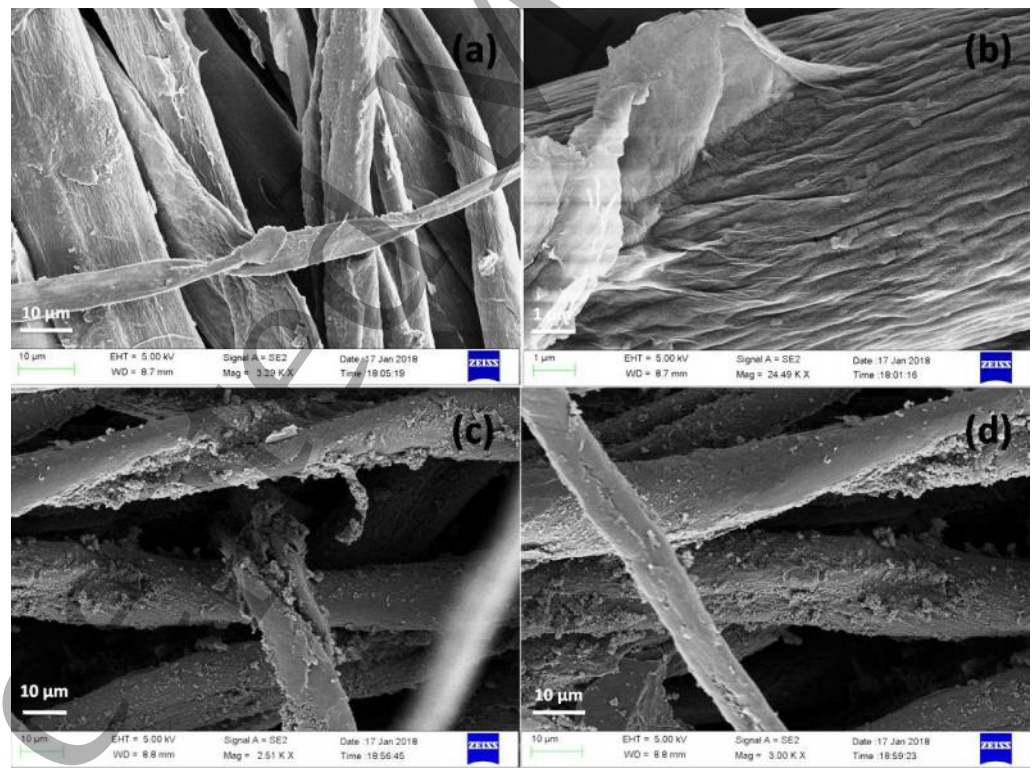

Fig.8. FE-SEM image of (a, b) rGO/MnO_2/cotton, (c, d) rGO/MnO2-PANi/cotton fabric

PANi was coated on rGO/MnO_2/cotton through in situ polymerization and PANi was covered the rGO/MnO_2 coated cotton fibers as thin layer, as shown in Fig.8. (c, d). Because the thick coating layers would block the diffusion of electrolyte ions to rGO and MnO_2 layers which results to low capacitance of the electrode. Finally, SEM images confirmed the transformation of morphology from rGO/cotton fabric to ternary sandwich structure of rGO/MnO_2/PANi/cotton fabrics.

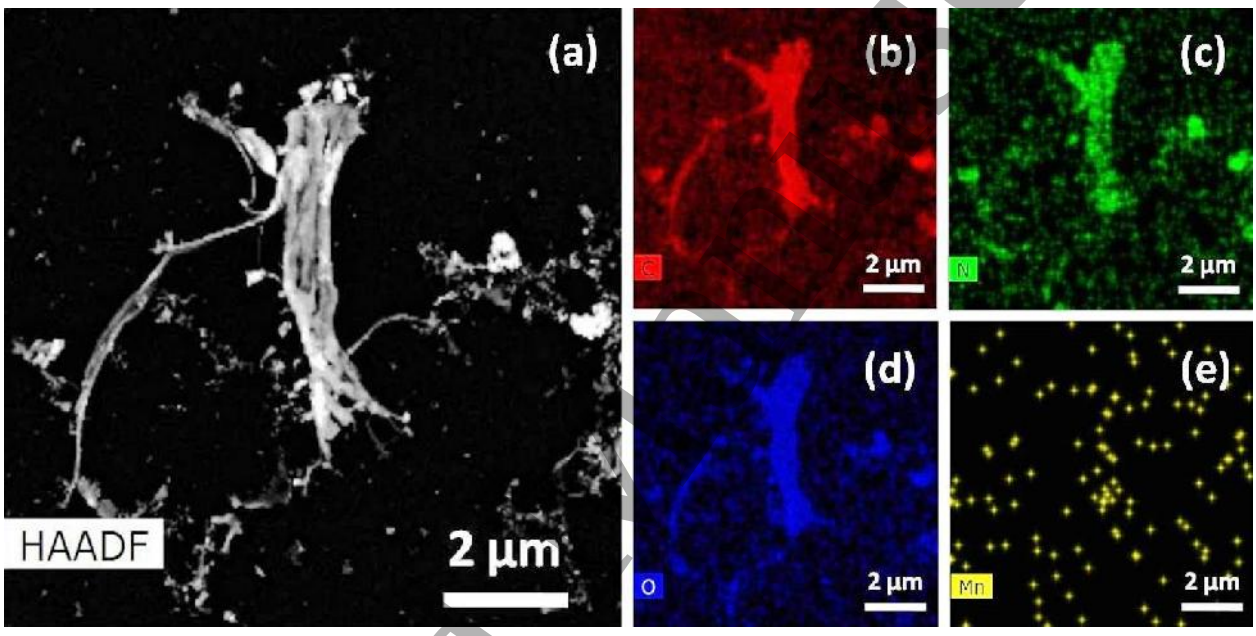

Fig.9. (a) HAADF-STEM image of rGO/MnO_2/PANi/cotton and element mappings of (b) C Ka1, (c) N Ka1, (d) O Ka1, (e) Mn Ka1

Energy-dispersive X-ray (EDX) spectroscopy was used to detect the composition of rGO/MnO_2/PANi/cotton fabric by elemental mapping technique. Fig.9. (a) shows the HAADF-STEM image of rGO/MnO_2/PANi/cotton fabric. It was observed that the presence of elements C, N, O, and Mn in rGO/MnO_2/PANi/cotton fabric which are shown in Fig. 9. (b-e). The presence of N confirms the PANi layer coated on the cotton fabric (Fig. 9. (c)), and the Mn (Fig. 9. (e)) indicates the existence of MnO_2 nanoparticles. Therefore, the elemental mapping confirms the ternary sandwich nanostructures of rGO/MnO_2/PANi/Cotton.

The overall electrochemical performance of the synthesized electrocatalyst are directly associated with specific surface area and pore diameter of the cotton samples. The N_2 adsorption

and desorption isotherms of rGO/MnO_2/PANi/cotton fabric as shown in Fig. 10(a) results indicates that type –IV with H3 hysteresis loop curves between (0- 1 p/p_o) relative pressure, which indicates the presence of mesopores and macropores features in samples. The pore size distribution of the rGO/MnO_2/PANi/cotton fabric was evaluated by Barret–Joyner–Halenda model (BJH) as shown in Fig. 10(b). [41]

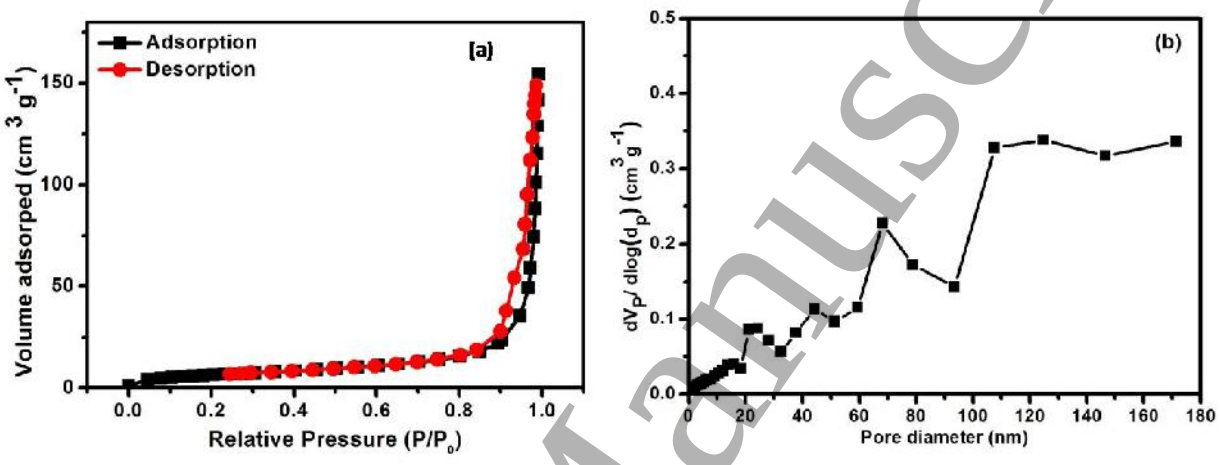

Fig.10. (a) Nitrogen adsorption and desorption isotherm of rGO/MnO_2/PANi/Cotton fabric electrode and (b). The Barret–Joyner–Halenda (BJH) pore size distribution plot of rGO/MnO_2/PANi/cotton fabric electrode

The result shows that the pore size distribution was mesoporous, and macroporous existed in rGO/MnO_2/PANi/cotton and it shows that BET surface area was 26 $m^2 g^{-1}$. This results indicates the polyaniline coated on the MnO_2 and graphene sheet. This architecture facilitates the transportation of ions and electrons in the matrix easily and thus enhances the electrochemical performances of the cotton electrode.

3.3. Electrochemical properties

The electrochemical properties were studied experimentally by a three-electrode cell system which consisted of 1 M H_2SO_4 aqueous solution as electrolyte, a Pt counter electrode, rGO/MnO_2/PANi cotton fabric working electrode, and an Ag/AgCl reference electrode. The Cyclic voltammetry (CV) and Galvanostatic charge-discharge cycle were studied for the developed cotton fabric electrodes. Fig.11 (a) shows CV curves of rGO/cotton,

rGO/MnO_2/cotton rGO/PANi/cotton, and rGO/MnO_2/PANi/cotton fabric electrodes in the range of –0.2 - 0.8 V at a scan rate of 20 mV s^{-1}. The rGO/cotton electrode does not show any rectangular shape CV curve. This may be due to the presence of functional groups such as –OH, –COOH, C–O–C in graphene oxide which were not removed completely in rGO. The rGO/MnO_2/cotton fabric electrode also does not show rectangular CV curve. This can be explained by the following reversible redox reaction mechanism

$$MnO_2 + H^+ + e^- \leftrightarrow MnOOH \quad \ldots\ldots\ldots\ldots\ldots\ldots(1)$$

The charge storage of MnO_2 coated cotton electrode in aqueous H_2SO_4 electrolyte is caused by the intercalation of proton during reduction (Mn^{4+} is reduced to Mn^{3+}) and de/intercalation upon oxidation (Mn^{3+} is oxidized to Mn^{4+}) in the electrode. The rGO/MnO_2/PANi/cotton electrode has pseudo-capacitance with largest capacitive current. This may be due to the redox reaction mechanism of PANi with two possible transitions such as leucoemeraldine-emaraldine and emeraldine-pernigraniline transition [42] as shown in Fig.12. Compared with rGO/PANi/Cotton electrode, the difference in peak potential of rGO/MnO_2/PANi/cotton electrode is decreased and this may be due to the redox reactions occur more reversibly. In Fig.11. (a), the closed area of hybrid of rGO/MnO_2/PANi components coated on cotton substrate is larger than that of rGO/cotton, rGO-MnO_2/cotton, and rGO-PANi/cotton electrode. This proved that the capacitive performance of rGO/MnO_2/PANi/cotton electrode is the best among the other electrodes.

Fig.11. (b) shows the Galvanostatic charge-discharge curves of rGO/cotton, rGO/MnO_2/cotton, and rGO/MnO_2/PANI/cotton electrodes at the discharge current density of 1.0 A g^{-1} in the potential range between -0.2 and +0.8 V vs. Ag/AgCl. It can be seen that all the electrodes show an asymmetric curves of charge-discharge cycles, which indicate the electrodes are pseudocapacitors.

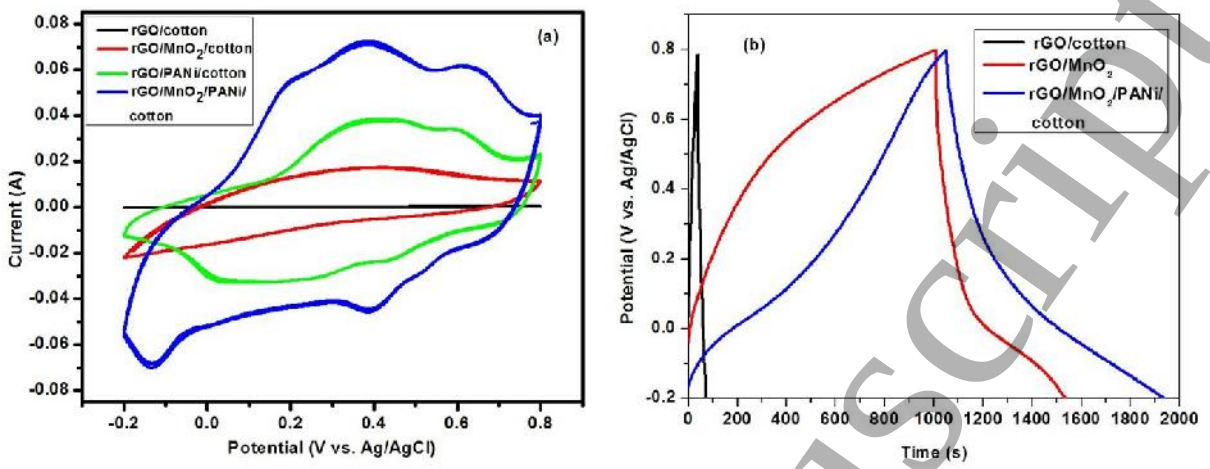

Fig.11. (a) CV curves of cotton electrodes in the potential range of –0.2 - 0.8 (V vs. Ag/AgCl) at a scan rate of 20 mV s^{-1}, (b) Galvanostatic charge-discharge curves of different cotton electrodes at 1 A g^{-1} current density

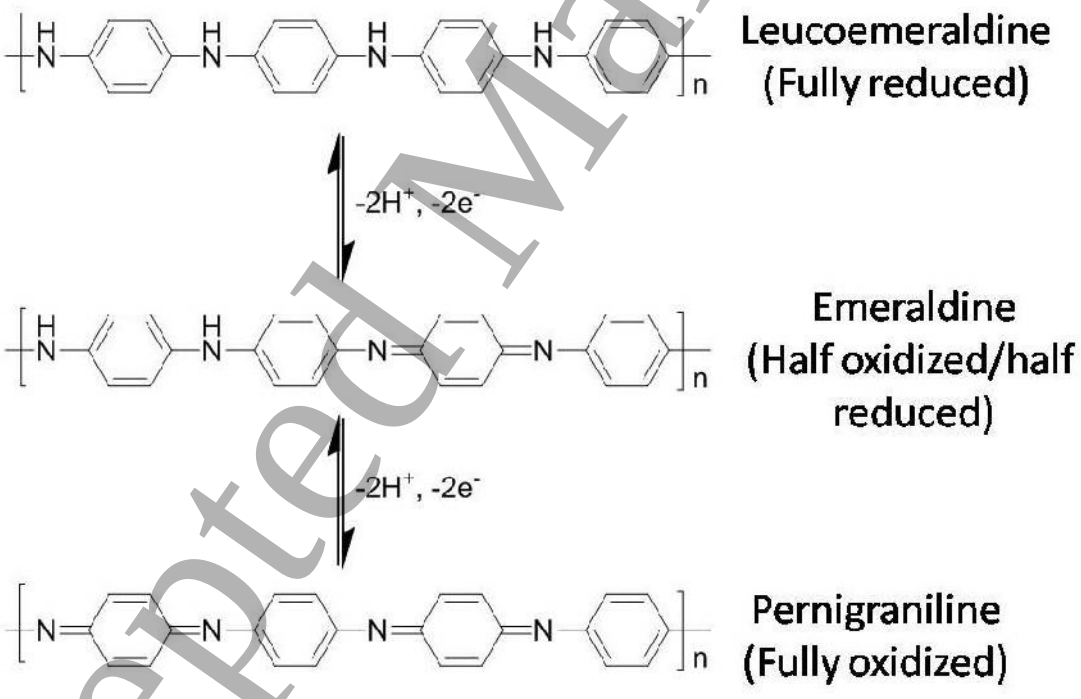

Fig.12. The schematic of electrochemical reaction mechanism of PANi

The specific capacitance is calculated by equation (2)

$$C_s = \frac{I\Delta t}{m\Delta V} \quad \text{.....(2)}$$

Where, C_{spec} is the specific capacitance (F g^{-1}), 'I' is the charge-discharge current density (A g^{-1}), ′Δt′ is the discharge time (s), 'm' is the mass of active material in the working electrode (g), and ′ΔV′is the potential window (V). The C_{spec} of developed cotton electrodes was calculated. The C_{spec} of rGO/MnO_2/PANi/cotton electrode is 888 F g^{-1} at 1.0 A g^{-1} current density, which is much higher compared to (136 F g^{-1}) of rGO and (523 F g^{-1}) of rGo/MnO_2. The specific capacitance of rGO/MnO_2/cotton electrode is improved because of the contribution of pseudocapacitive behavior from MnO_2. Further, the addition of PANi coating layer to rGO/MnO_2/cotton drastically enhance the capacitance. This may be due to the synergic effect of PANi with rGO and MnO_2. It can be explained that a thin PANi coating layer acts as a protective layer on rGO/MnO_2/cotton fabric to restrain MnO_2 nanoparticles and rGO from dissolution in H_2SO_4 acidic electrolyte.

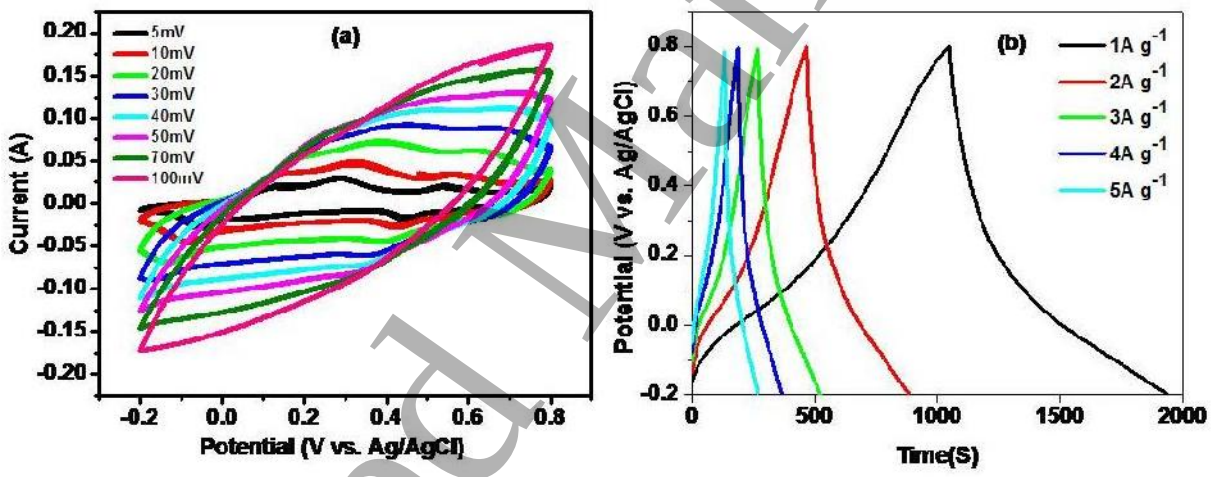

Fig.13. (a) CV curves of rGO/MnO_2/PANi/cotton electrode at different scan rates. (b) Galvano static charge-discharge curves of rGO/MnO_2/PANi/cotton electrode at different current density ranging from 1 to 5 A g^{-1} at potential of -0.2 to 0.8 (V vs.Ag/AgCl)..

Fig.13 (a) shows CV curves of rGO/MnO_2/PANi/cotton electrode at scan rates ranging from 5mV s^{-1} to 100 mV s^{-1}. There is some redox peaks observed due to the pseudo capacitance by the presence of MnO_2 and PANi. It is observed that the cathodic peaks shift to positive side and the anodic peaks shift to negative side when the scan rate increases from 5 to 100 mV s^{-1}, due to the resistance of the electrode material. The Galvanostatic charge-discharge curves of

rGO/MnO_2/PANi/cotton electrode at different current ranges between 1.0 and 5 A g^{-1} is shown in Fig. 13. (b).

The dependence of areal and volumetric specific capacitances on current density range of 1 – 25 A g^{-1}) of rGO/MnO2/PANi/cotton electrode with the size of 2 cm^2 area and 0.05 cm thickness was then studied (Fig.14). The maximal areal and volumetric specific capacitance of 444.0 F cm^{-2} and 403.6 F cm^{-3} at current density of 1 A g^{-1} decreased to 125.0 F cm^{-2} and 114.5 F cm^{-3} at current density of 25 A g^{-1} respectively. This shows that an increase in current density decreases the specific capacitance gradually of rGO/MnO2/PANi/cotton electrode.

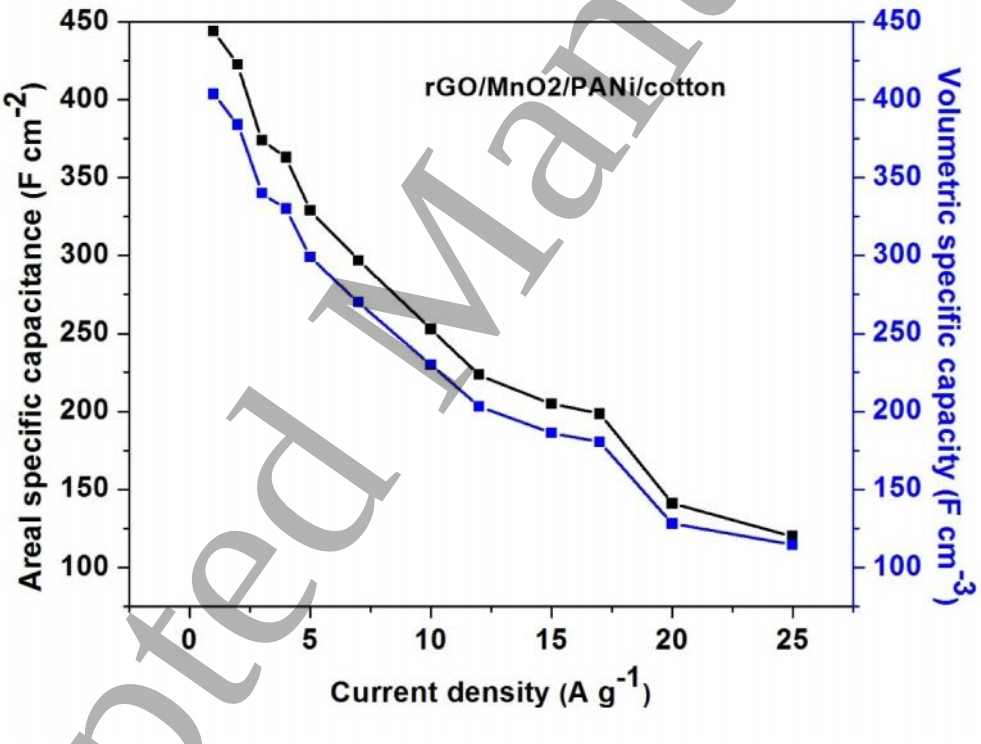

Fig.14. Dependence of Areal and volumetric specific capacitance on current density (1 – 25 A g^{-1}) of rGO/MnO2/PANi/cotton electrode.

The main objective of the Electrochemical Impedance Spectroscopic studies is to evaluate ion diffusions in the electrode and electrolyte interface. The electrochemical impedance and resistance of the electrode material can be represented by Nyquist plot (Fig.15). It is the sum of real (Z'), and imaginary (Z") components which represent the resistance and capacitance of the

electrode, respectively. The shape of Nyquist plot includes a semicircle region lying on the Z'-axis followed by a straight line. The semicircle region represents the electron-transfer-limited process and the straight line region corresponds to the diffusional-limited electron-transfer process.

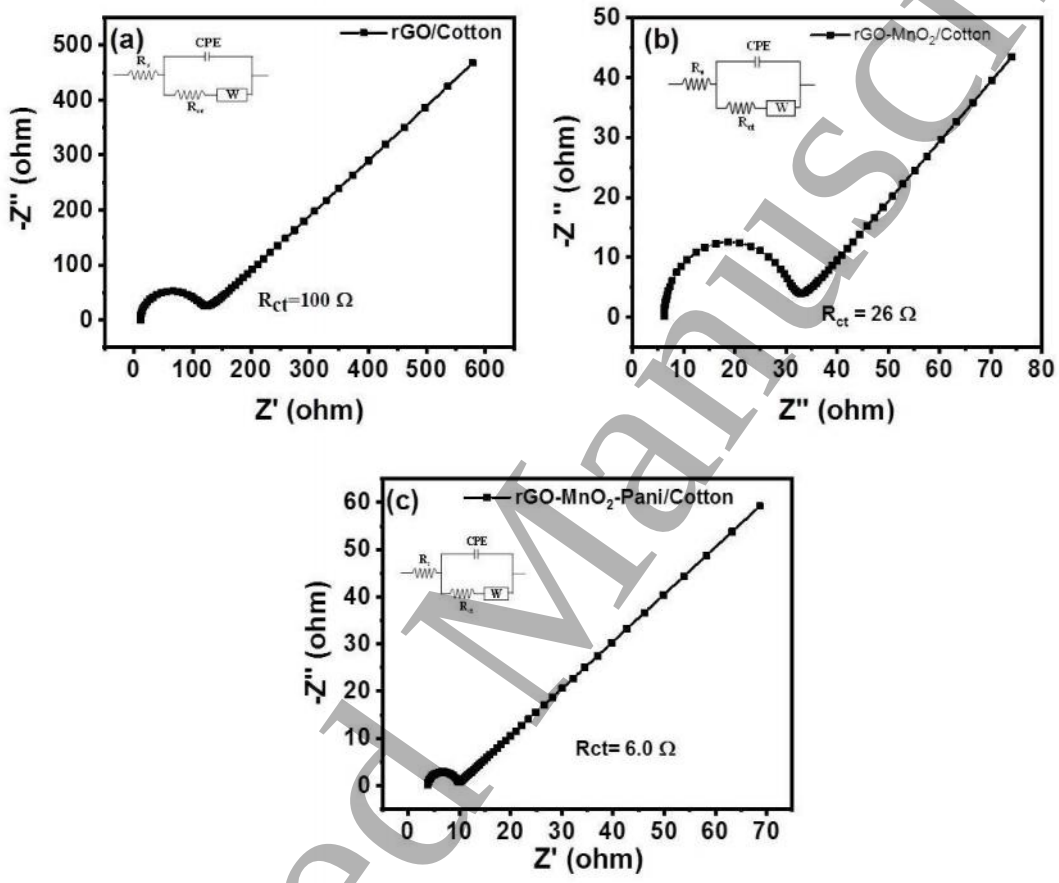

Fig.15. Nyquist plots of (a) rGO/Cotton, (b) rGO/MnO_2/Cotton, and (c) rGO/MnO_2/PANi/Cotton fabric electrode

From Nyquist plots (Fig.15. (a-c)), rGO/cotton shows a semicircle at high frequency region which is followed by a straight line at low frequency region. The rGO/MnO_2/cotton also forms a semicircle at low frequency and this may be due to the addition of MnO_2. It can be observed that the rGO/MnO_2/PANi/cotton fabric electrode displays a semicircle at high frequency region and a more vertical straight line at low frequency region compared to rGO/Cotton and rGO/MnO_2/cotton electrodes. This indicates that rGO/MnO_2/PANi/cotton electrode has low Faradaic charge transfer resistances and a faster ion (H^+) diffusion rate which leads the material

to have better capacitive behavior. The resistance of rGO/cotton, rGO/MnO_2/cotton, and rGO/MnO_2/PANi/cotton were measured to be 100.0 Ω, 26.0 Ω, and 6.0 Ω respectively. There was a decrease in resistance observed due to the addition of MnO_2 and PANi to rGO/cotton electrode.

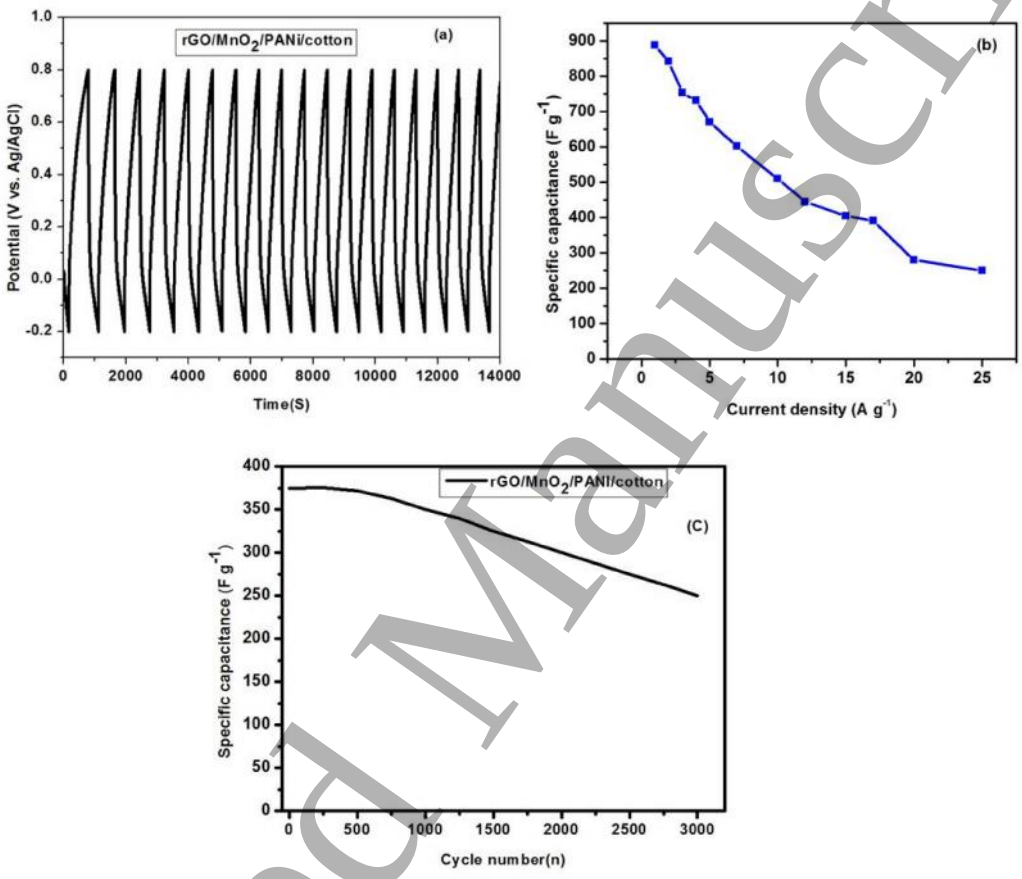

Fig.16. (a) Galvanostatic charge/discharge curves of rGO/MnO_2/PANi/cotton electrode at current density of 2 A g^{-1} at potential of -0.2 to 0.8 (V vs.Ag/AgCl), (b) Plot of specific capacitance of rGO/MnO_2/PANi/cotton electrode at different discharge currents (1 – 25 A g^{-1}) in 1 M H_2SO_4 aqueous electrolyte solution, and (c) Cycling stability of rGO/MnO_2/PANi/cotton electrode at a current density of 15 A g^{-1}.

Galvanostatic charge/discharge curve (Fig.16. (a)) of cotton electrode was recorded at a discharge current density of 2 A g^{-1} for 12000 seconds. Fig.16. (b) shows the specific capacitance of rGO/MnO_2/PANi/cotton electrode at different discharge currents ranging between

1 and 25 A g^{-1}. It can be seen that the specific capacitance decreases from 888 F g^{-1} to 252 F g^{-1} with increasing current density (1.0 A g^{-1} to 25.0 A g^{-1}).

Table.2. Comparison of electrochemical properties between as-fabricated rGO/MnO_2/PANI electrode and reported electrodes in literature.

Electrode material	**Specific capacitance**	**Current density/ Scan rate**	**Electrolyte (M)**	**Stability (cycles)**	**Reference**
rGO/CCF	87.53 mF cm^{-2}	2.0 mV s^{-1} (scan rate)	6 M KOH	89.82 % (1000)	[6]
MnO2/rGO@C	329.4 mA h g^{-1}	100 mA g^{-1}	Ethylene carbonate (EC)-dimethyl carbonate (DMC)-diethyl carbonate (DEC) (1:1:1)	93.7 % (70)	[7]
PANI/RGO/PETC	1293 F g^{-1}	1 A g^{-1}	H_2SO_4 (1 mol L^{-1})	95% (3000)	[14]
Graphene/Cotton	40 F g^{-1}	0.85 A g^{-1}	Na_2SO_4 (1 mol. L^{-1})	90% (1000)	[15]
RGO/Cu_2O/TiO_2	80 F g^{-1}	0.2 A g^{-1}	6 M KOH	100% (1000)	[21]
PANi/GR	922 Fg^{-1}	10 mV s^{-1} (scan rate)	1 M H_2SO_4	90% (1000)	[30]
PANI-HS36@ERGO	614 F g^{-1}	1.0 A g^{-1}	1 M H_2SO_4	90% (500)	[31]
PANi-*g*-rGO	250 F g^{-1}	10 mV s^{-1} (scan rate)	1 M H_2SO_4	-	[33]
GO/PANI	425 F g^{-1}	0.2 A g^{-1}	1 M H_2SO_4	83% (500)	[34]
RGO/PANi	361 F g^{-1}	0.3 A g^{-1}	1 M H_2SO_4	80% (1000)	[36]
RuO_2/GNs	365 F g-1	20 mV s^{-1} (scan rate)	1 M H_2SO_4	90% (6000)	[37]
rGO/MnO_2/PANi/cotton	888 F g^{-1}	1.0 A g^{-1}	1 M H_2SO_4	70% (3000) at 15 A g^{-1}	This work

The comparison between as fabricated electrode and the other electrode materials for supercapacitors reported in literature is shown in Table.2. The obtained specific capacitance of 888 F g^{-1} at a current density of 1 A g^{-1} is higher than the reported rGO/cotton based electrode in

literature. [31] Also, the long-cycle stability of supercapacitor is an important requirement for energy storage applications. Fig.16.(c) shows the curve of specific capacitance versus cycle number. The rGO/MnO_2/PANi/cotton electrode retains around 70% after 3000 cycles at a high discharge current of 15 A g^{-1}. This shows that the ternary materials coated cotton electrode has higher cycling stability even at high discharge current density. Therefore, the rGO/MnO_2/PANi/cotton electrode can be an excellent electrode material for supercapacitors in energy storage application.

4. Conclusion

In this work, the unique ternary materials rGO/MnO_2/PANi coated cotton electrodes have been successfully fabricated by step-wise synthesis procedure. The electrochemical studies of rGO/MnO_2/PANi/cotton electrode confirm that PANi layer can protect rGO and MnO_2 particle on cotton surface and also increase the specific capacitance of the electrode. The fabricated rGO/MnO_2/PANi/cotton fabric as working electrode was tested in a three electrode electrochemical cell with 1 M H_2SO_4 electrolyte for energy storage application. For the rGO/MnO_2/PANi/cotton electrode, the maximum specific capacitance value of 888 F g^{-1} and minimum of 250 F g^{-1} was achieved at the current density of 1.0 A g^{-1} and 25 A g^{-1} respectively. It retained around 70% of initial specific capacitance after 3000 charge-discharge cycles at high discharge current of 15 A g^{-1}, which demonstrates the ternary materials coated cotton electrode with excellent specific capacitance and good cycle stability. This proves that rGO/MnO_2/PANi/cotton fabric will be the suitable electrode material for supercapacitor in energy storage applications.

Acknowledgements

The authors thank Indian Institute of Science for providing laboratory facilities and Jimma University for providing financial support to carry out the research work in India.

REFERENCES

[1] Vishakha K, Jaehong L, Juree H, Seulah L, Sanggeun L, Jungmok S, Chandreswar M and Taeyoon L2015 Review: Textile-Based Electronic Components for Energy Applications: Principles, Problems, and Perspective *Nanomat.* **5**, 1493–1531

[2] Shengli Z, Enis K H, Li W, Qihui Q, Andrew T H, Andrew I M, Ramakrishna S, Andrew K N, Yuan C2016 Textile energy storage: Structural design concepts, material selection and future perspectives *Energy Stor Mat*. **3**, 123–139

[3] Hao T, Wang W and Yu D2018 A Flexible Cotton-Based Supercapacitor Electrode with High Stability Prepared by Multiwalled CNTs/PANI *J Elec Mater*.**47,** 4108

[4] Zan G, Clifton B, Ningning S, Yunya Z, and Jingjing L 2016 Cotton-textile-enabled flexible self-sustaining power packs via roll-to-roll fabrication *Nature Commun*. **7** 11586

[5] Minmin H, Tao H, Renfei C, Jinxing Y, Cong C, Chao Z, and Xiaohui W 2018MXene-coated silk-derived carbon cloth toward flexible electrode for supercapacitor application *J Energy Chem*. **27** 161–166

[6] Qianlong Z, Xingke Y, Zhongquan W, and Chunyang J 2015A three-dimensional flexible supercapacitor with enhanced performance based on lightweight, conductive graphene-cotton fabric electrode *J Power Sources*. **296** 186-196

[7] Mingwei T, Minzhi D, Lijun Q, Kun Z, Hongliang L, Shifeng Z, and Dongdong L 2016 Conductive reduced graphene oxide/MnO_2 carbonized cotton fabrics with enhanced electro -chemical, -heating, and –mechanical properties *J Power Sources*. **326** 428-437

[8] Xiao Y L, Kai X W, and Jie S C 2016 Template-directed metal oxides for electrochemical energy storage *Energy Stor Mater*.**3** 1–17

[9] Ling B K, Jing Z, Jing J, Yong C L, and Long K 2008 MWNTs/PANI composite materials prepared by in-situ chemical oxidative polymerization for supercapacitor electrode*J Mater Sci*. **43** 3664–3669

[10] Li Y and Chen C 2017 Polyaniline/carbon nanotubes-decorated activated carbon fiber felt as high-performance, free-standing and flexible supercapacitor electrodes *J Mater Sci*. **52** 12348

[11] Tamai H, Hakoda M,Shiono T and Yasuda H 2007 Preparation of polyaniline coated activated carbon and their electrode performance for supercapacitor*J Mater Sci*. **42**1293–1298

[12] Jie X, Daxiang W, Ye Y, Wei W, Shaojin G, Ruina L, Xiaojun W, Li L, and Weilin X 2015Polypyrrole-coated cotton fabrics for flexible supercapacitor electrodes prepared using CuO nanoparticles as template *Cellulose.***22** 1355–1363

[13] Ji E L, Seon J P, Oh S K, Hyeon W S, Jyongsik J, and Hyeonseok Y 2014 Systematic investigation on charge storage behaviour of multidimensional poly (3,4ethylenedioxythiophene) nanostructures *RSC Adv*.**4** 37529–37535

[14] Fu S, Shao W B, Quan Z, Mei X G, Si L, and Yi H P 2016 Fabrication of Polyaniline/Graphene/Polyester Textile Electrode Materials for Flexible Supercapacitors with High Capacitance and Cycling Stability *Chem. Asian J*.**11** 1906 –1912

[15] Ling L X, Mei X G, Si L and Shao W B 2015 Graphene/cotton composite fabrics as flexible electrode materials for electrochemical capacitors *RSC Adv*.**5** 25244–25249

[16] Chun J, Hai T W, Ya N L, Xiao H K, Ping L, Jia N Z, Li N J, Shao W B, and Quan Z 2018 High-performance yarn electrode materials enhanced by surface modifications of cotton fibers with graphene sheets and polyaniline nanowire arrays for all-solid-state supercapacitors *Electrochim Acta*.**270**205-214

[17] Wen W L, Xing B Y, Jun W L, Chao P and Qun J X 2012 Flexible and conductive nanocomposite electrode based on graphene sheets and cotton cloth for supercapacitor *J. Mater. Chem.***22** 17245–17253

[18] Kena C, Qingrong W, Zhiqiang N, and Jun C 2018 Review Graphene-based materials for flexible energy storage devices *J Energy Chem*. 27, (2018) 12–24

[19] Xiaoyu S, Shuanghao Z, Zhong S W, and Xinhe B 2018 Review Recent advances of graphene-based materials for high-performance and new-concept supercapacitors *J Energy Chem.* **27**25–42

[20] Xiaoning T, Mingwei T, Lijun Q, Shifeng Z, Xiaoqing G, Guangting H, Kaikai S, Xili H, Yujiao W, and Xiaoqi X 2015 Functionalization of cotton fabric with graphene oxide nanosheet and polyaniline for conductive and UV blocking properties *Synth Metals.***202** 82–88

[21] Dongming L, Yaping L, Jinlong L, Haibo F, Dong Q, Sanjun P, Jianbo J, and Youcai L 2013 One-step solution-phase synthesis of a novel RGO–Cu_2O–TiO_2 ternary nanocomposite with excellent cycling stability for supercapacitors *J Alloy and Comp.***581** 303–307

[22] Hyun K K, Sang H P, Seung B Y, Chang W L, Jun H J, Kwang C R, and Kwang B K 2014 In Situ Synthesis of Three-Dimensional Self-Assembled Metal Oxide Reduced Graphene Oxide Architecture *Chem. Mater*, **26** 4838–4843

[23] Suk W L, Seong M B, Chang W L, Cherno J, Daniel A F, Bae K K, Xiao Q Y, Kyung W N, and Kwang B K 2014 Structural Changes in Reduced Graphene Oxide upon MnO_2 Deposition by the Redox Reaction between Carbon and Permanganate Ions*J. Phys. Chem. C*.**118** 2834-2843

[24] Tianyu L, Lauren F, Minghao Y, Hanyu W, Teng Z, Xihong L, Yexiang T, and Yat L 2014 Polyaniline and Polypyrrole Pseudocapacitor Electrodes with Excellent Cycling Stability*ACS Nano Lett.***14** 2522-2527

[25] Ravi M A P, José J A E, Fernando A G S, and Helinando P O 2018 Multifunctional wearable electronic textiles using cotton fibers with polypyrrole and carbon nanotubes, *ACS Appl. Mater. Interfaces.***10**13783–13795

[26] Qianhui W, Ming C, Shishuang W, Xiue Z, Long H, and Guowang D 2016 Preparation of sandwich-like ternary hierarchical nanosheets manganese dioxide/polyaniline/reduced graphene oxide as electrode material for supercapacitor, *Chem Eng J*.**304** 29–38

[27] Lianmei Liu, Wei Weng, Jing Zhang, Xunliang Cheng, Ning Liu, Junjie Yang, Xin Ding 2016 Flexible supercapacitor with a record high areal specific capacitance based on a tuned porous fabric *J. Mater. Chem. A.* **4** 12981-12986

[28] Wenjie L, Shishuang W, Qianhui W, Long H, Xiue Z, ChaoY, and Ming C 2016 Fabrication of ternary hierarchical nanofibers MnO_2/PANI/CNT and theirs application in electrochemical supercapacitors, *ChemEng Sci*.**156** 178-185

[29] Anukul K T, Ram B C, Mandira M, and Malati M 2017Fairly improved pseudocapacitance of PTP/PANI/TiO_2nanohybrid composite electrode material for supercapacitor applications *Ionics*.**24** 1-12

[30] Fei P D, Jing J W, Chak Y T, Chi P T, Xiao L X, and Ka F Y 2013 Enhanced Electrochemical Capacitance of Polyaniline/graphene Hybrid Nanosheets with Graphene as Templates *Comp. Part B: Eng.***53** 376-381

[31] Wei F, Chao Z, Weng W T, Kumari P P, Chaobin H, and Tianxi L 2013Graphene-Wrapped Polyaniline Hollow Spheres As Novel Hybrid Electrode Materials for Supercapacitor Applications *ACS Appl. Mater. Interfaces*. **5** 3382–3391

[32] Jiliang C and Chaoxia W 2018 Highly conductive and flexible silk fabric via electrostatic self assemble between reduced graphene oxide and polyaniline *Org Electronics.***55** 26–34

[33] Nanjundan A K, Hyun J C, Yeon R S, Dong W C, and Jong B B 2012 Polyaniline-Grafted Reduced Graphene Oxide for Efficient Electrochemical Supercapacitors, *ACS Nano.***6**1715-1723

[34] Guiheng X, Nan W, Junyi W, Leilei L, Jianan Z, Zhimin C, and Qun X 2012 Preparation of Graphene Oxide/Polyaniline Nanocomposite with Assistance of Supercritical Carbon Dioxide for Supercapacitor Electrodes *ACS Ind. Eng. Chem. Res.***51** 14390-14398

[35] Xinhong Z, Lanfeng L, Shanmu D, Xiao C, Pengxian H, Hongxia X, Jianhua Y, Chaoqun S, Zhihong L, and Guanglei C 2012 A renewable bamboo carbon/polyaniline composite for a high-performance supercapacitor electrode material *J Solid State Electrochem.***16**877–882

[36] Jintao Z and Zhao X S 2012 Conducting Polymers Directly Coated on Reduced Graphene Oxide Sheets as High-Performance Supercapacitor Electrodes *J. Phys. Chem. C,* **116**5420-5426

[37] Rakhi R B, Chen W, Cha D and Alshareef H N 2011High performance supercapacitors using metal oxide anchored graphene nanosheet electrodes *J. Mater. Chem.***21** 16197–16204

[38] Yong J, Xuetao L, Zheng J, Li L, Qiliang M, Minghong W, Yuliang C, and Bing Z 2015 Flexible of multiwalled carbon nanotubes/manganese dioxide nanoflake textiles for high-performance electrochemical capacitors *ElectrochimicaActa.***153** 246–253

[39] Qiufeng M, Kefeng C, Yuanxun C, and Lidong C 2016 Review Research progress on conducting polymer based supercapacitor electrode materials *Nano energy*, **36** 268-285

[40] Ramakrishnan S, Dhakshnamoorthy M, Jelmy E J, Vasanthakumari R and Nikhil K K 2014 Synthesis and characterization of graphene oxide–polyimide nanofiber composites *RSC Adv.***4** 9743-9749

[41] Nilesh R. Chodankar,a Girish S. Gund,a Deepak P. Dubalb and Chandrakant D. Lokhande 2014 Alcohol mediated growth of α-MnO2 thin films from KMnO4 precursor for high performance supercapacitors, RSC Adv. **4** 61503-61513

[42] Xueliang L, Yunfu L, Wei G, Jiejie C, Wen xiang H, and Fang fang P 2014 Synthesis of spherical PANI particles via chemical polymerization in ionic liquid for high-performance supercapacitors *Electrochim Acta.***135** 550–557